An Interdomain Linker Increases the Thermostability and Decreases the Calcium Affinity of the Calmodulin N-Domain†

Brenda R. Sorensen, Laurel A. Faga, Rainbo Hultman, and Madeline A. Shea*

Department of Biochemistry, University of Iowa College of Medicine, Iowa City, Iowa 52242-1109

Received August 23, 2001; Revised Manuscript Received October 31, 2001

ABSTRACT: A hydrophobic core is a widely accepted determinant of protein stability. However, regulatory proteins undergoing ligand-induced conformational switching may expose interior residues to solvent and cannot afford to be extremely rigid. Optimizing the energetic balance between stability and binding is challenging. The addition of five interdomain residues to rat and *Paramecium* calmodulin N-domain fragments (residues 1−75) increased their thermostability by 9 °C and lowered their calcium affinity by a factor of 4. This demonstrates that the flexible linker regulates functional properties as well as tethering the neighboring domains and that protein stability may be increased markedly by minor modifications of the C-terminus. The sensitivity of this domain to few and conservative variations in helices A and D (D2E, S17A, T70S and M71L) is demonstrated by the rat CaM fragments having lower stability and higher calcium affinity than fragments of the same length derived from *Paramecium* CaM.

The network of intramolecular contacts in a regulatory protein achieves a balance between rigidity needed for stability and flexibility required for function. However, the stability and ligand binding properties of an individual domain within a multidomain protein may be context-dependent, modified by energetic interactions that cannot be predicted on the basis of sequence homology with similar domains. This complicates the design of regulatory proteins and the formulation of hypotheses regarding newly identified sequences.

This is exemplified by the diversity found within the large family of EF-hand calcium-binding proteins (*1*). Despite a high degree of structural homology between the helix−loop−helix units comprising each hand (*2*), these proteins differ in their affinities for metals, cooperativity of binding, thermostabilities, and degrees of calcium-induced conformational change (*3*−*6*). Calmodulin (CaM)[1] demonstrates how two paired EF-hand domains can be linked but have different stabilities (*7*−*9*) and widely separated ligand affinities (*10*−*13*) despite the similarity of their sequences and structures (*14*) (see Figure 1).

In this work, we focus on the N-domain of CaM as a model system for understanding determinants of thermostability and calcium affinity. By comparing recombinant fragments of rat CaM (rCaM) and *Paramecium* CaM (PCaM) ending at position 75 (CaM_{1-75}) and 80 (CaM_{1-80}; see Figure 2), we explore the effects of adding a five-residue "tail" and of natural sequence variations. These studies indicate that the addition of five residues to the C-terminus of the N-domain decreased its calcium affinity by a factor of 4 and increased its stability by almost 10 °C. We propose that the linker makes distal contacts with helix A, stabilizing the relative orientation of the A and D helices.

This is the first demonstration of the use of a C-terminal tail to stabilize an EF-hand protein. It shows that solvent-exposed regions may have a large effect on stability. The added residues comprise the next five residues of the calmodulin sequence, an interdomain linker that had been viewed as a passive barrier to diffusion of the two domains. This linker may play an unrecognized regulatory role for functional control of the N-domain. By decreasing its affinity for calcium, the linker would contribute to increasing the concentration of calcium required to trigger physiological responses mediated by this domain. The findings have general applicability to the design of protein maquettes and the study of other four-helix bundle proteins.

MATERIALS AND METHODS

Cloning and Purification. The DNA encoding the *Paramecium* calmodulin fragments ($PCaM_{1-75}$ and $PCaM_{1-80}$) and rat calmodulin fragments ($rCaM_{1-75}$ and $rCaM_{1-80}$) was cloned into the T7-7 vector (*15*, *16*) using standard techniques (*7*) and overexpressed in *Escherichia coli* Lys-S cells (U.S. Biochemicals, Cleveland, OH) as described previously (*17*). Recombinant CaM_{1-75} and CaM_{1-80} fragments were purified using phenyl Sepharose CL-4B (Amersham Pharmacia Biotech, Piscataway, NJ) chromatography as described previously (*17*). Fractions containing CaM were further purified on a DEAE-Sephacel anion exchange column (Amersham Pharmacia Biotech) using a 100 to 700 mM NaCl gradient in 20 mM Tris, 1 mM EDTA, and 1 mM DTT

† These studies were supported by grants to M.A.S. from the National Institutes of Health (RO1 GM 5001).

* To whom correspondence should be addressed. Telephone: (319) 335-7885. Fax: (319) 335-9570. E-mail: madeline-shea@uiowa.edu.

[1] Abbreviations: CaM, calmodulin; CD, circular dichroism; DEAE, diethylaminoethyl; EGTA, ethylene glycol bis(2-aminoethyl ether)-*N*,*N*,*N*′,*N*′-tetraacetic acid; NTA, nitrilotriacetic acid; pCa, $-\log[Ca^{2+}]_{free}$; PCaM, *Paramecium* calmodulin; rCaM, rat calmodulin; RP-HPLC, reversed phase high-performance liquid chromatography.

10.1021/bi011718+ CCC: $22.00
Published on Web 12/05/2001

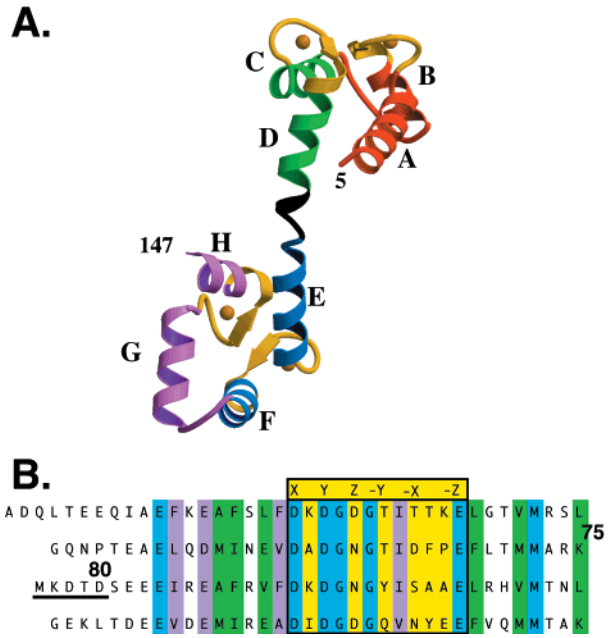

FIGURE 1: (A) Ribbon diagram of $(Ca^{2+})_4$-CaM as determined by X-ray crystallography. Coordinates for residues 5−147 were resolved (*45*) and reported as Protein Data Bank (*46*) entry 3CLN. The four 12-residue calcium-binding sites (I−IV) are highlighted in yellow, and each EF-hand lettered A−H is colored orange (EF-hand I), green (EF-hand II), blue (EF-hand III), or purple (EF-hand IV). The region in the central helix shown to be flexible by NMR (*47*) is depicted as a random coil, and residues 76−80 are highlighted in black. These drawings were created using MOLSCRIPT (*48*) and RASTER3D (*49*). (B) Amino acid sequence of rCaM aligned to illustrate sequence similarity among the four EF-hands. The calcium-binding sites are enclosed within a yellow box, and positions within each site involved in chelating calcium ion are labeled X, Y, Z, −Y, −X, and −Z (*50*, *51*). Sequences that are identical in each EF-hand are highlighted in blue; those conserved in EF-hands I and III, or II and IV, are highlighted in green, and those that retain similar chemical properties in all four EF-hands are highlighted in purple. Residues 76−80 are underlined to illustrate the variable region between CaM_{1-75} and CaM_{1-80}.

(pH 8.0). All of the N-domain fragments were at least 97% pure as judged by RP-HPLC. Purified fractions were dialyzed against 50 mM HEPES and 100 mM KCl (pH 7.40), and aliquots were stored at −20 °C.

Thermal Unfolding. Thermal unfolding studies were performed on an AVIV 62DS CD spectrometer equipped with a thermoelectric temperature controller and an immersible thermocouple, accurate to ±0.4 °C. Proteins were diluted to 10 μM in a total volume of 3 mL of 2 mM HEPES, 100 mM KCl, 5 mM NTA, and 0.05 mM EGTA (pH 7.40). Samples were denatured with increasing temperature from 5 to 95 °C at a rate of 1 °C/min. The spectral signal at 222 nm was averaged for 20 s every 30 s and stored with experimental measurements of temperature. Samples were rapidly cooled to 5 °C; the percent renaturation for all samples was ≥98.0 ± 1.0%.

The normalized ellipticity data from thermal denaturation of CaM N-domain fragments were fit to two-state and three-state models of unfolding (*18*, *19*) using *nonlin* (*20*) as described previously (*7*, *21*). The contribution of each species to the overall observed spectral signal was estimated on the basis of its fractional population (f_N, f_I, and f_U). This value can be determined on the basis of the equilibrium constants for unfolding between each species [$K_i = \exp(-\Delta G_i/RT)$]

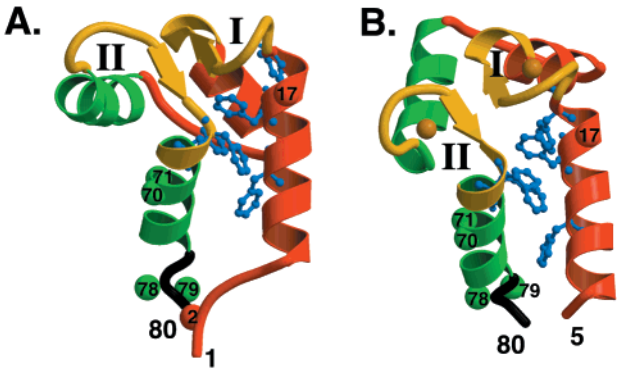

FIGURE 2: Ribbon diagrams of (A) apo CaM residues 1−80 as determined by NMR and (B) $(Ca^{2+})_4$-CaM residues 5−80 as determined by X-ray crystallography. Coordinates were taken from Protein Data Bank entries (A) 1CFD (*14*) and (B) 3CLN (*45*). The 12-residue calcium binding sites (I and II) are highlighted in yellow, and the five phenylalanine side chains monitored by fluorescence (see Figure 4) are shown in blue. Residues 76−80 are highlighted in black. The positions of residues that differ between rCaM and PCaM are numbered and shown as colored spheres where the sequence differences are as follows (rat and *Paramecium*): 2 (D and E), 17 (S and A), 70 (T and S), 71 (M and L), 78 (D and E), and 79 (T and Q). These drawings were created using MOLSCRIPT (*48*) and RASTER3D (*49*).

which in turn can be expressed at any temperature for any transition using a modified Gibbs−Helmholtz equation:

$$\Delta G_i = \Delta H_i^\circ\left(1 - \frac{T}{T_{m_i}}\right) + \Delta C_{p_i}\left[T - T_{m_i} - T\left(\ln\frac{T}{T_{m_i}}\right)\right] \quad (1)$$

where ΔH_i° is the van't Hoff enthalpy and ΔC_{p_i} is the heat capacity for transition i (i.e., N−I or I−U transition). When the unfolding data were fit to a two-state model, all parameters were allowed to vary; however, in the three-state analysis, ΔC_p was fixed to 0. Criteria for "goodness of fit" included (a) the value of the square root of variance, (b) the values of asymmetric 65% confidence intervals, (c) examination of any trends in the distribution of residuals, (d) the magnitude of the span of the residuals, and (e) the absolute value of elements of the correlation matrix (*20*). In all cases, the two-state model best described the data.

Calcium Titrations. Calcium titrations of CaM fragments were monitored by observing the change in phenylalanine fluorescence using an SLM 4800 instrument as described previously (*21*). Samples of 6 μM protein were incubated in 50 mM HEPES, 100 mM KCl, 0.05 mM EGTA, 5 mM NTA, and 0.1 μM Oregon Green (pH 7.40, 22 °C). The free calcium concentration was determined throughout the titration by the degree of saturation of Oregon Green 488 BAPTA-5N as described previously (*17*) using a K_d for Oregon Green 488 BAPTA-5N of 29.60 μM determined in 50 mM HEPES and 100 mM KCl (pH 7.40, 22 °C). Titrations for each fragment were repeated three times except for $rCaM_{1-80}$, which was repeated twice. Values reported in Table 2 are averages of these trials. The Gibbs free energies of calcium binding were obtained from fits of the titration data as described previously (*7*, *17*, *22*−*24*).

RESULTS

Effect of Length on Stability. The stability of apo rat and *Paramecium* CaM_{1-75} and CaM_{1-80} was assessed by moni-

Table 1: Thermal Denaturation of Apo CaM Fragments

protein	T_m (°C)	$\Delta H_{VH}°$ (kcal/mol)	ΔC_p (cal/K·mol)	√var
$rCaM_{1-75}$[a]	50.25 ± 0.08	46.65 ± 0.41	566 ± 139	0.215
$rCaM_{1-80}$[a]	59.31 ± 0.05	52.75 ± 0.47	1246 ± 76	0.234
Δ	9.06	6.10		
$PCaM_{1-75}$[a]	55.79 ± 0.07	51.19 ± 0.58	1120 ± 172	0.319
$PCaM_{1-80}$[a]	64.65 ± 0.06	55.95 ± 0.67	1325 ± 52	0.254
Δ	8.86	4.76		

[a] Values resolved from fitting the data to a two-state model for unfolding (eq 1).

Table 2: Free Energies of Calcium Binding

protein	ΔG_1 (kcal/mol)	ΔG_2 (kcal/mol)	ΔG_c (kcal/mol)	√var
$rCaM_{1-75}$[a]	−5.90 ± 0.22	−13.84 ± 0.08	−2.85 ± 0.40	0.012 ± 0.003
$rCaM_{1-80}$[a]	−5.95 ± 0.25	−13.05 ± 0.10	−1.98 ± 0.60	0.013 ± 0.009
Δ		0.79		
$PCaM_{1-75}$[a]	−6.12 ± 0.09	−12.99 ± 0.04	−1.56 ± 0.14	0.011 ± 0.001
$PCaM_{1-80}$[a]	−6.11 ± 0.02	−12.46 ± 0.07	−1.05 ± 0.05	0.008 ± 0.002
Δ		0.53		

[a] Values resolved from fitting the data to a two-site Adair function (sites may be nonequivalent and cooperative) for ligand binding (*7*, *17*, *22*−*24*).

toring the temperature-dependent change in ellipticity at 222 nm of rCaM (Figure 3A) and PCaM (Figure 3B). The unfolding data were fit to two-state and three-state models as described previously (*7*, *21*). In all cases, the two-state model best described the data. The resolved values of melting temperature, enthalpy, and heat capacity are reported in Table 1.

The differences in thermodynamic properties indicated that increasing the length of the CaM fragment from 75 to 80 residues was stabilizing, suggesting that residues in this region participate in secondary and tertiary structure contacts. For rCaM, the melting temperature (T_m) increased from 50.25 to 59.31 °C (ΔT_m = 9.06 °C) and the ΔH of unfolding increased by 6.10 kcal/mol. For PCaM, the T_m increased from 55.79 to 64.65 °C (ΔT_m = 8.86 °C) and the ΔH of unfolding increased by 4.76 kcal/mol. Thus, the incremental effects of adding five residues to the CaM_{1-75} fragments were comparable for rat and *Paramecium* CaM.

Effect of Length on Calcium Binding. We monitored equilibrium calcium binding titrations of rat and *Paramecium* CaM_{1-75} and CaM_{1-80} using calcium-dependent changes in fluorescence intensity. Although these proteins do not contain tryptophan or tyrosine, the five naturally occurring phenylalanine residues (positions 12, 16, 19, 65, and 68) serve as optical probes (*21*). Figure 2 illustrates their positions in the tertiary structure of apo CaM (Figure 2A) and $(Ca^{2+})_4$-CaM (Figure 2B).

When calcium bound, the phenylalanine fluorescence intensity decreased in both rCaM (Figure 4A) and PCaM (Figure 4B) fragments. The free energies of calcium binding resolved from these binding isotherms are shown in Table 2. For each species, the pairs of curves (CaM_{1-75} vs CaM_{1-80}) were well separated. Increasing the length of the domain decreased the affinity for calcium binding to sites I and II by 0.79 kcal/mol in rCaM and 0.53 kcal/mol in PCaM. These differences ($\Delta\Delta G_2$) are significantly larger than the confidence intervals for ΔG_2 (0.02−0.05 kcal/mol) determined from analysis of individual titrations and the standard deviation of the average values (see Table 2) obtained by averaging the results from multiple determinations.

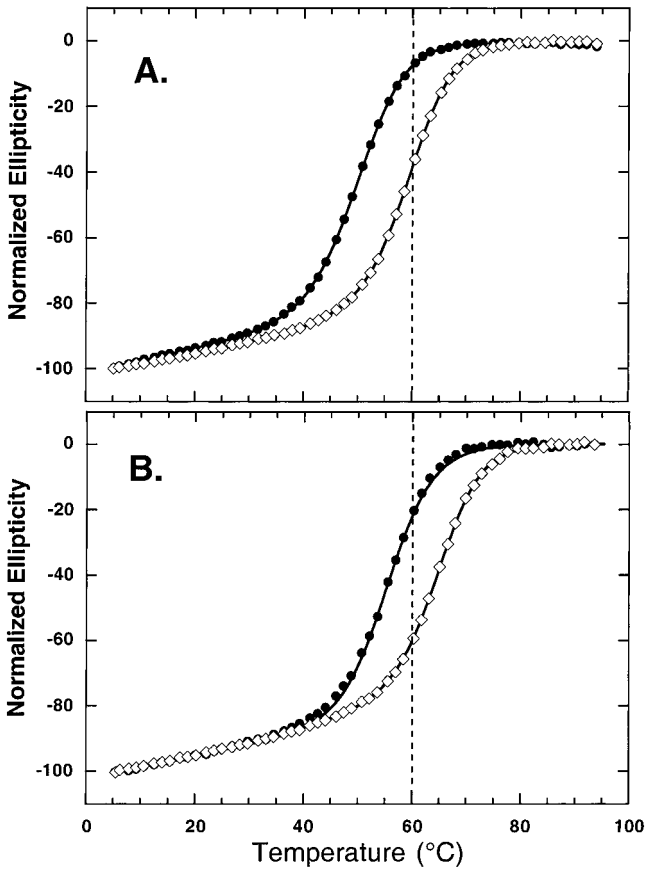

FIGURE 3: Thermal unfolding of (A) rCaM and (B) PCaM residues 1−75 (●) and 1−80 (◇) as monitored by circular dichroism at 222 nm. Lines through the data were simulated on the basis of the resolved parameters from a nonlinear least-squares analysis of the data using a two-state model for unfolding (eq 1). These data are representative of results observed in at least three determinations. Dashed lines facilitate comparison of melting curves.

Effect of 5−*7% Nonidentity.* The primary sequence of $PCaM_{1-148}$ is 88% identical to that of $rCaM_{1-148}$ with the greatest deviation observed in residues 81−148 (i.e., in the C-terminal domain). The percent identity of the first 80 residues in the sequences is 93%; when the first 75 residues are compared, it increases further to 95%. Thus, the range of nonidentity is 5−7%. Comparing results for $rCaM_{1-75}$ and $PCaM_{1-75}$ indicated that the conservative substitutions at positions 2 (D_{rCaM} and E_{PCaM}) and 17 (S_{rCaM} and A_{PCaM}) in helix A and positions 70 (T_{rCaM} and S_{PCaM}) and 71 (M_{rCaM} and L_{PCaM}) in helix D increased the thermostability of $PCaM_{1-75}$ relative to that of $rCaM_{1-75}$ by 5.54 °C (see Figure 3 and Table 1) and decreased the calcium affinity by 0.85 kcal/mol (see Figure 4 and Table 2).

The extension of CaM_{1-75} by five residues introduced two additional amino acid differences at positions 78 (D_{rCaM} and E_{PCaM}) and 79 (T_{rCaM} and Q_{PCaM}) for a total of six residue variations between $rCaM_{1-80}$ and $PCaM_{1-80}$. These differences increased the thermostability of $PCaM_{1-80}$ relative to that of $rCaM_{1-80}$ by 5.34 °C and decreased the calcium affinity by 0.59 kcal/mol. These species-specific differences between CaM_{1-80} are significant relative to the confidence intervals on the individual determinations and standard deviations for the averages.

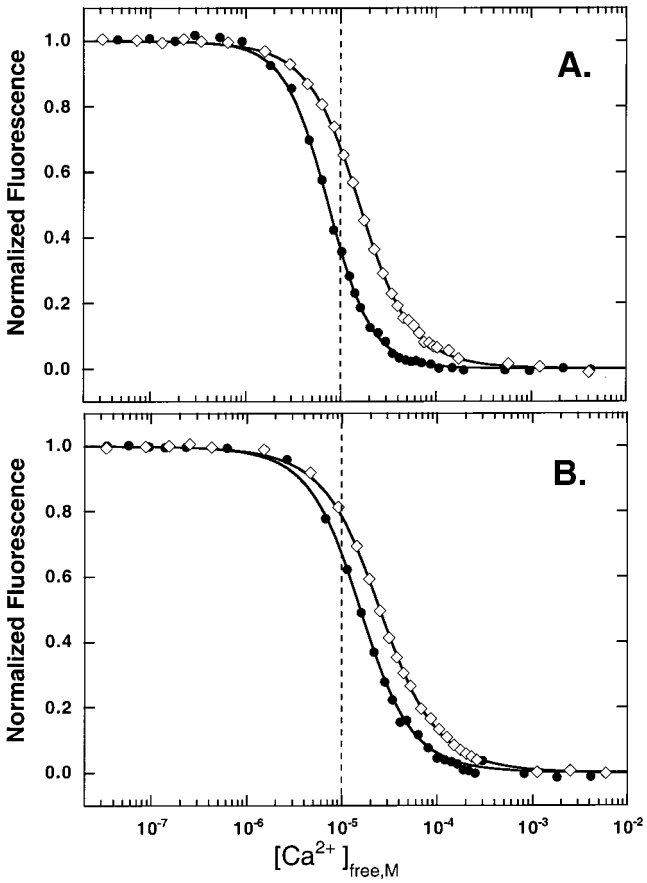

FIGURE 4: Phenylalanine fluorescence of (A) rCaM and (B) PCaM residues 1−75 (●) and 1−80 (◇). Lines through the data were simulated on the basis of the resolved parameters from a nonlinear least-squares analysis of the data using a two-site heterogeneous and cooperative model for ligand binding (*7*, *17*, *22*−*24*). These data are representative of results observed in at least two determinations. Dashed lines facilitate comparison of fluorescence curves.

DISCUSSION

Thermostabilities and calcium affinities of individual EF-hand domains are known to correlate with their degree of calcium-induced conformational change (for a review, see ref *4*). Calcium "buffers" such as calbindin D_{9K} and calpain are more stable, have a lower affinity for calcium, and undergo very little conformational change upon binding calcium compared to regulatory EF-hand proteins such as calmodulin and troponin C which undergo large calcium-induced conformational changes (*4*). Our findings for CaM_{1-75} and CaM_{1-80} from two species demonstrate that tail residues may have a large impact on the stability of a domain comprised of two EF-hands. It is of interest to consider the specific roles of these additional residues.

Domain Stability. Many investigators are attempting to elucidate the rules that govern protein folding and stability (e.g., refs *25*−*28*). Although folding is driven primarily by the entropically favorable burial of apolar side chains, it is also influenced by the relative exposure of the peptide backbone (*29*). Studies of thermostable proteins (including those from thermophilic organisms) indicate that protein stability can be enhanced by hydrogen bond formation, electrostatic interactions, and surface loop deletions (*30*−*32*). Although these classes of molecular contacts are present in most proteins, their relative contributions to stability are

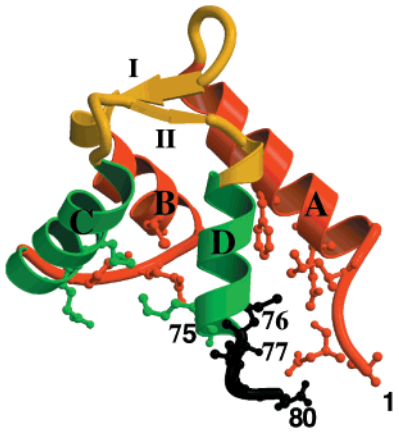

FIGURE 5: Ribbon diagram of distal contacts made with Lys75, Met76, Lys77, Asp78, and Asp80 in the NMR solution structure of apo CaM [PDB entry 1CFD (*14*)]. Only residues 1−80 are illustrated. Residues Glu78 and Thr79 in the flexible tether (shown in black) had contacts only with local residues in the sequence of residues 1−80 and so are not highlighted. The 12-residue calcium binding sites (I and II) are colored yellow. For clarity, residues in EF-hands I (helices A and B) and II (helices C and D) are colored orange and green, respectively. These drawings were created using MOLSCRIPT (*48*) and RASTER3D (*49*).

dependent on the exact sequence and structure of an individual protein (*33*).

To explore the molecular basis for the increase in stability of apo CaM_{1-80} relative to apo CaM_{1-75}, we used the OCA browser [http://bioinfo.weizmann.ac.il:8500/ (*34*)] to analyze inter-residue contacts. This analysis showed that in the structure of apo CaM (PDB entry 1CFD) determined using NMR, Lys75 engages in eight contacts with the preceding 74 residues. Five of these are with residues in and between helices B and C (residues 36, 41, 43, 47, and 51; see Figure 5), and the remainder are local (i.e., with immediately preceding residues 71, 72, and 74). In comparison, the tail residues (Met76, Lys77, Asp78, Thr79, and Asp80) engage in a total of 37 contacts with other residues in the sequence of residues 1−80. Most of these (*26*) are local contacts. However, Met76, Lys77, and Asp81 make a total of seven contacts with residues close to the N-terminus of the sequence: positions 1, 2, 4, 8, and 12 in helix A (see Figure 5). The ability of apo CaM_{1-80} to engage in these additional contacts with helix A may play a significant role in the 9 °C increase in its stability relative to that of apo CaM_{1-75}.

The increase in stability of the apo N-domain conferred by residues 76−80 correlated well with a decrease in the proteolytic susceptibility of CaM_{1-80}. For rat CaM, the scissile bond between Arg37 and Ser38 in helix B of $rCaM_{1-80}$ was ∼10 times less susceptible than the same bond in $rCaM_{1-75}$ as observed in thrombin footprinting (*7*, *22*, *24*) under apo conditions (C. Strong and M. A. Shea, data not shown). A difference also was observed for PCaM, where the Arg37−Ser38 bond was ∼3 times less susceptible in $PCaM_{1-80}$ than in $PCaM_{1-75}$. Thus, regardless of sequence, susceptibility decreased when the C-terminus was extended beyond Lys75.

Calcium Affinity. When calcium binds to CaM, the two helices in each EF-hand rearrange from a parallel to nearly perpendicular orientation. The four-helix bundle makes a transition from a "closed" to an "open" conformation (see Figure 2) (*2*, *3*, *35*). Using the OCA browser to analyze the

contacts made by Met76, Lys77, Asp78, Thr79, and Asp80 in a structure of $(Ca^{2+})_4$-CaM (PDB entry 3CLN) determined crystallographically, we found that six of the seven contacts with helix A observed in the apo structure were lost. The exception was the contact between Met76 and Phe12. In CaM_{1-80}, calcium-induced conformational switching must disrupt these contacts, while CaM_{1-75} has fewer constraints on its tertiary structure. This may account for the higher calcium affinity of CaM_{1-75}.

This view is consistent with mutational studies of calmodulin. Grabarek and co-workers engineered a disulfide bridge between position 41 in the linker between helices B and C and position 75 in helix D and found that the apo N-domain is locked into a closed conformation that results in a lower calcium affinity of sites I and II (*6*). Similar conclusions were reached by Desjarlais and co-workers (*5*), who further mutagenized a triply mutated form of vertebrate CaM_{1-78} to investigate which amino acids account for the functional differences between calmodulin and calbindin. The significance of these interactions was also demonstrated in a mutant form of $PCaM_{1-75}$ where a substitution of Glu for Gly at position 40 decreased the stability of the fragment by ~18 °C, increased its affinity by ~0.5 kcal/mol, and increased its Stokes radius by ~0.7 Å (*21*).

Species-Specific Differences. The C-terminal tail residues (76−80) stabilize the apo N-domain of CaM by contributing to a network of intramolecular contacts that maintain a closed conformation in the absence of calcium. Differences between the properties of fragments of equal length derived from *Paramecium* and rat N-domain sequences demonstrate that few and conservative variations in this highly conserved domain also contribute to differences in stability and calcium affinity. The four sequence differences between $PCaM_{1-75}$ and $rCaM_{1-75}$ are located in helices A and D, consistent with the hypothesis that contacts between these two helices have a significant impact on stability.

Four-Helix Bundle Proteins. Although the stabilizing effect of C-terminal tail residues on EF-hand proteins has not been explored systematically, this phenomenon has been observed in several other four-helix bundle repressor proteins, tumor suppressors, and enzymes. In these examples, the functional consequences of this stabilization varied. In one case, the tail increased stability but had minimal impact on function [e.g., the tumor suppressor PTEN (*36*)], while in others, the tail stabilized otherwise unstable repressor proteins or their domain fragments [e.g., P22 Arc, the N-domain of λ cI, and CopR (*37*−*40*)].

Previous studies demonstrated that $rCaM_{1-75}$ is well-folded as judged by circular dichroism (*7*) and NMR (*41*). It is thermally stable with a T_m only 2.7 °C lower than that of the same domain within $rCaM_{1-148}$ (*7*). Thus, CaM_{1-75} does not fall into the class of protein fragments that were terminated prematurely and required a tail for rescuing a poorly folded chain. Adding residues 76−80 from the interdomain linker of CaM increased its thermostability but compromised the calcium binding function of both rCaM and PCaM N-domain fragments. This is similar to the case of aldehyde dehydrogenase where a five-amino acid tail was found to reduce activity by 30% (*42*).

Biological Consequences. Because the tail being "added" to CaM_{1-75} is part of the naturally occurring sequence, it may be a component of optimizing the physiological function of the protein given the similarity of the original building blocks (four EF-hand units). The energetic penalty conferred by this five-residue C-terminal tail suggests that covalent linkage of the C-domain to the N-domain contributes to reduction of the calcium affinity of sites I and II in the N-domain relative to the affinity of sites III and IV in the C-domain. This would contribute to separating the median ligand activity of each domain and would have an impact on the molecular switch that regulates the calcium-induced conformational changes that are critical for CaM to regulate its protein targets.

CONCLUSIONS

On the basis of internal sequence homology of CaM (Figure 1), Lys75 is in a position analogous to Lys148, the final residue of CaM. It appears to result from a gene duplication event and is a prime candidate for serving as the final residue of the N-domain. However, Figures 3 and 4 showed that the addition of the next five residues in the CaM sequence had a large impact on the domain stability and calcium affinity of sites I and II. From this study alone, it is not clear whether a single peptide bond may be assigned as the boundary between the N- and C-domains of full-length CaM. A criterion for such an assignment would be that the energetic properties of the resulting complementary fragments would recapitulate those observed in CaM_{1-148} over the full range of ionic equilibria in which it operates. However, the properties of the interdomain linker region (and, therefore, the boundary between the domains) may be calcium-dependent. This has been suggested by a 10−20-fold increase in the susceptibility of Lys75 to trypsin proteolysis upon binding calcium to sites III and IV (*43*, *44*) and analysis of the network of intramolecular contacts within high-resolution structures. To address this issue, studies are underway to vary the length of the N-domain and compare its energetic properties to those ascribed to the N-domain within CaM_{1-148}.

ACKNOWLEDGMENT

We thank J. B. Alexander Ross for assistance in optimizing the performance of the SLM 4800 instrument used in these studies, Cynthia Strong for thrombin footprinting analysis of CaM_{1-75} and CaM_{1-80}, and the reviewers for their helpful suggestions.

REFERENCES

1. Nakayama, S., and Kretsinger, R. H. (1994) *Annu. Rev. Biophys. Biomol. Struct. 23*, 473−507.
2. Yap, K. L., Ames, J. B., Swindells, M. B., and Ikura, M. (1999) *Proteins 37*, 499−507.
3. Nelson, M. R., and Chazin, W. J. (1998) *Protein Sci. 7*, 270−282.
4. Berggård, T., Julenius, K., Ogard, A., Drakenberg, T., and Linse, S. (2001) *Biochemistry 40*, 1257−1264.
5. Ababou, A., and Desjarlais, J. R. (2001) *Protein Sci. 10*, 301−312.
6. Tan, R.-Y., Mabuchi, Y., and Grabarek, Z. (1996) *J. Biol. Chem. 271*, 7479−7483.
7. Sorensen, B. R., and Shea, M. A. (1998) *Biochemistry 37*, 4244−4253.
8. Masino, L., Martin, S. R., and Bayley, P. M. (2000) *Protein Sci. 9*, 1519−1529.
9. Tsalkova, T. N., and Privalov, P. L. (1985) *J. Mol. Biol. 181*, 533−544.

10. Klevit, R. E., Dalgarno, D. C., Levine, B. A., and Williams, R. J. P. (1984) *Eur. J. Biochem. 139*, 109−114.
11. Crouch, T. H., and Klee, C. B. (1980) *Biochemistry 19*, 3692−3698.
12. Wang, C.-L. A. (1985) *Biochem. Biophys. Res. Commun. 130*, 426−430.
13. Seamon, K. B. (1980) *Biochemistry 19*, 207−215.
14. Kuboniwa, H., Tjandra, N., Grzesiek, S., Ren, H., Klee, C. B., and Bax, A. (1995) *Nat. Struct. Biol. 2*, 768−776.
15. Studier, F. W., Rosenberg, A. H., Dunn, J. J., and Dubendorff, J. W. (1990) *Methods Enzymol. 185*, 60−89.
16. Tabor, S., and Richardson, C. C. (1985) *Proc. Natl. Acad. Sci. U.S.A. 82*, 1074−1078.
17. Pedigo, S., and Shea, M. A. (1995) *Biochemistry 34*, 1179−1196.
18. Eftink, M. R., Ionescu, R., Ramsay, G. D., Wong, C., Wu, J. Q., and Maki, A. H. (1996) *Biochemistry 35*, 8084−8094.
19. Carra, J. H., Anderson, E. A., and Privalov, P. L. (1994) *Biochemistry 33*, 10842−10850.
20. Johnson, M. L., and Frasier, S. G. (1985) *Methods Enzymol. 117*, 301−342.
21. VanScyoc, W. S., and Shea, M. A. (2001) *Protein Sci. 10*, 1758−1768.
22. Shea, M. A., Verhoeven, A. S., and Pedigo, S. (1996) *Biochemistry 35*, 2943−2957.
23. Jaren, O. R., Harmon, S., Chen, A. F., and Shea, M. A. (2000) *Biochemistry 39*, 6881−6890.
24. Shea, M. A., Sorensen, B. R., Pedigo, S., and Verhoeven, A. (2000) *Methods Enzymol. 323*, 254−301.
25. Liang, J., and Dill, K. A. (2001) *Biophys. J. 81*, 751−766.
26. Li, R., and Woodward, C. (1999) *Protein Sci. 8*, 1571−1590.
27. Socci, N. D., Onuchic, J. N., and Wolynes, P. G. (1998) *Proteins 32*, 136−158.
28. Sivaraman, T., Arrington, C. B., and Robertson, A. D. (2001) *Nat. Struct. Biol. 8*, 331−333.
29. Bolen, D. W., and Baskakov, I. V. (2001) *J. Mol. Biol. 310*, 955−963.
30. Vogt, J., Woell, S., and Argos, P. (1997) *J. Mol. Biol. 269*, 631−643.
31. Jaenicke, R., and Böhm, G. (1998) *Curr. Opin. Struct. Biol. 8*, 738−748.
32. Thompson, M. J., and Eisenberg, D. (1999) *J. Mol. Biol. 290*, 595−604.
33. Matthews, B. W. (1993) *Annu. Rev. Biochem. 62*, 139−160.
34. Sobolev, V., Sorokine, A., Prilusky, J., Abola, E. E., and Edelman, M. (1999) *Bioinformatics 15*, 327−332.
35. Swindells, M. B., and Ikura, M. (1996) *Nat. Struct. Biol. 3*, 501−504.
36. Vazquez, F., Ramaswamy, S., Nakamura, N., and Sellers, W. R. (2000) *Mol. Cell. Biol. 20*, 5010−5018.
37. Milla, M. E., Brown, B. M., and Sauer, R. T. (1993) *Protein Sci. 2*, 2198−2205.
38. Milla, M. E., Brown, B. M., and Sauer, R. T. (1994) *Struct. Biol. 1*, 518−523.
39. Parsell, D. A., and Sauer, R. T. (1989) *J. Biol. Chem. 264*, 7590−7595.
40. Kuhn, K., Steinmetzer, K., and Brantl, S. (2000) *J. Mol. Biol. 300*, 1021−1031.
41. Lee, S. Y., and Klevit, R. E. (2000) *Biochemistry 39*, 4225−4230.
42. Rodriguez-Zavala, J., and Weiner, H. (2001) *Chem.-Biol. Interact. 130−132*, 151−160.
43. Mackall, J., and Klee, C. B. (1991) *Biochemistry 30*, 7242−7247.
44. Giedroc, D. P., Puett, D., Sinha, S. K., and Brew, K. (1987) *Arch. Biochem. Biophys. 252*, 136−144.
45. Babu, Y. S., Bugg, C. E., and Cook, W. J. (1988) *J. Mol. Biol. 204*, 191−204.
46. Berman, H. M., Westbrook, J., Feng, Z., Gilliland, G., Bhat, T. N., Weissig, H., Shindyalov, I. N., and Bourne, P. E. (2000) *Nucleic Acids Res. 28*, 235−242.
47. Ikura, M., Spera, S., Barbato, G., Kay, L. E., Krinks, M., and Bax, A. (1991) *Biochemistry 30*, 9216−9228.
48. Kraulis, P. J. (1991) *J. Appl. Crystallogr. 24*, 946−950.
49. Merritt, E. A., and Bacon, D. J. (1997) *Methods Enzymol 277*, 505−524.
50. Kretsinger, R. H., and Nockold, C. E. (1973) *J. Biol. Chem. 215*, 3313−3326.
51. Strynadka, N. C. J., and James, M. N. G. (1989) *Annu. Rev. Biochem. 58*, 951−998.

BI011718+